RESEARCH ARTICLE | OCTOBER 26 2023

Ultrafast spectral diffusion of GaN defect single photon emitters ⊕⊘

Yifei Geng **थ** ⊚ ; Kazuki Nomoto ⊚

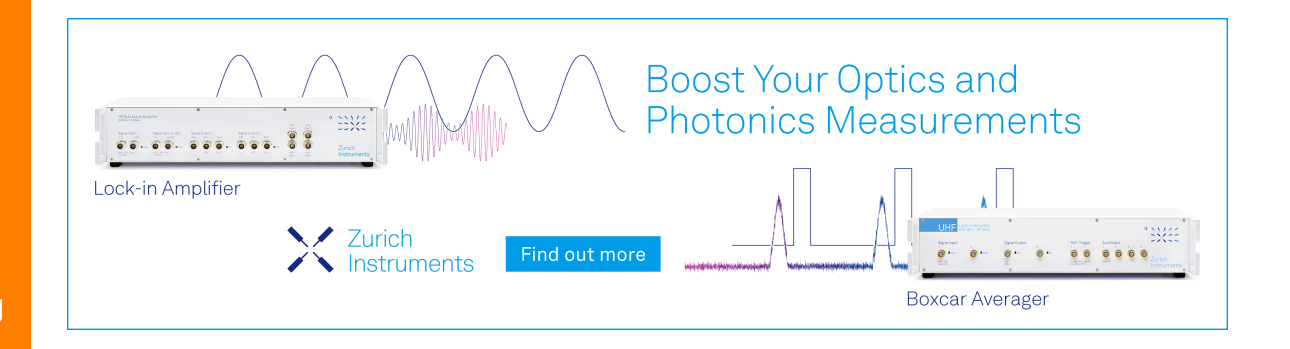


Appl. Phys. Lett. 123, 174002 (2023)

https://doi.org/10.1063/5.0171855









Ultrafast spectral diffusion of GaN defect single photon emitters •

Cite as: Appl. Phys. Lett. **123**, 174002 (2023); doi: 10.1063/5.0171855 Submitted: 10 August 2023 · Accepted: 9 October 2023 · Published Online: 26 October 2023







Yifei Geng^{a)} 🕞 and Kazuki Nomoto 🕞

AFFILIATIONS

School of Electrical and Computer Engineering, Cornell University, Ithaca, New York 14853, USA

a) Author to whom correspondence should be addressed: yg474@cornell.edu

ABSTRACT

Defect-based single photon emitters play an important role in quantum information technologies. Quantum emitters in technologically mature direct wide bandgap semiconductors, such as nitrides, are attractive for on-chip photonic integration. GaN has recently been reported to host bright and photostable defect single photon emitters in the 600-700 nm wavelength range. Spectral diffusion caused by local electric field fluctuation around the emitter limits the photon indistinguishability, which is a key requirement for quantum applications. In this work, we investigate the spectral diffusion properties of GaN defect emitters integrated with a solid immersion lens, employing both spectral domain and time domain techniques through spectroscopy and photon autocorrelation measurements at cryogenic temperature. Our results show that the GaN defect emitter at 10 K exhibits a Gaussian line shape with a linewidth of \sim 1 meV while the spectral diffusion characteristic time falls within the range of a few hundred nanoseconds to a few microseconds. We study the dependency of the spectral diffusion rate and Gaussian linewidth on the excitation laser power. Our work provides insight into the ultrafast spectral diffusion in GaN defect-based single photon emitter systems and contributes toward harnessing the potential of these emitters for applications, especially for indistinguishable single photon generation.

Published under an exclusive license by AIP Publishing. https://doi.org/10.1063/5.0171855

Single photon emitters (SPEs) are a fundamental building block in quantum information technologies. SPEs, which are bright, photostable, linearly polarized, of narrow emission linewidth and easy to be integrated in technically mature materials are especially desired. Recently, GaN has been reported to host bright and photostable defect SPEs in the 600-700 nm wavelength range.²⁻⁴ As a technically mature, direct wide bandgap semiconductor, GaN finds extensive applications in photonic devices, 5-7 semiconductor RF, and power devices.8-Consequently, GaN defect SPEs hold special significance for on-chip photonic integration compared to other defect emitters, such as color centers in diamond or defect SPEs in 2D materials. Various properties of GaN defect SPEs, such as photoluminescence (PL) spectrum,² defect-phonon coupling mechanism, 12 optical dipole structure and orientation, 13 and optically detected magnetic resonance, 14 have been studied. However, the origin of these defects is still elusive. Point defects, such as impurity atoms or impurity atom-vacancy complexes 12,15 and electron states localized at dislocations or stacking faults,² are suggested as potential candidates.

The photon indistinguishability of SPEs plays a crucial role in enabling secure quantum communication, reliable quantum computing, accurate quantum metrology, and efficient generation of entangled states. ¹⁶ Spectral diffusion refers to the phenomenon wherein the

emission energy of SPEs changes over time due to local electric field fluctuations around the emitter.¹⁷ It typically restricts photon indistinguishability at low temperatures when the phonon-induced spectral broadening is negligible. At cryogenic temperatures, spectral diffusion induced spectral line shape is known to be Gaussian, and the linewidth is a measure of the strength of the local field fluctuation. 12,18 However, capturing the rapid dynamics of spectral diffusion, which typically occurs on timescales ranging from nanoseconds to milliseconds is challenging using regular spectroscopy. Photon autocorrelation spectroscopy, which converts spectral fluctuations into intensity fluctuations, harnesses the sub-nanosecond time resolution of the Hanbury Brown and Twiss (HBT) interferometer to reveal the rapid dynamics of spectral diffusion.¹⁹ Ultrafast spectral diffusion timescales have been studied in various SPE platforms, such as quantum dots, 19-23 NV centers in diamond, ^{24,25} and defects in 2D materials like hBN. ²⁶ However, the spectral diffusion effect in GaN defect-based SPE systems has not been investigated.

In this work, we study the spectral diffusion effect of GaN defect SPEs integrated with a solid immersion lens, employing both spectral domain and time domain techniques through spectroscopy and photon autocorrelation measurements at cryogenic temperature. Our experimental results show that the spectral diffusion induced Gaussian

linewidth is about 1 meV at 10 K. Applying the photon autocorrelation technique, we select a narrow spectral window of the SPE emission light using the monochromator to enter the HBT interferometer. The measured ultrafast spectral diffusion timescale falls within the range of a few hundred nanoseconds to a few microseconds. We then investigate the dependence of the spectral diffusion rate and Gaussian linewidth on the excitation laser power. Our results demonstrate that the spectral diffusion rate exhibits a linear dependence on the excitation power, while the Gaussian linewidth shows a nearly square root relationship with the excitation power. Our work provides insight into the ultrafast spectral diffusion in GaN defect-based SPE systems.

A custom-built confocal scanning microscope setup together with a monochromator and an HBT interferometer was used for the spectral diffusion study as shown in Fig. 1(a). The GaN sample was mounted inside a helium flow cryostat. A 532 nm continuous wave

laser was focused on the sample to excite the defect emitter through the cryostat window using an objective lens (NA = 0.7) with a correction collar. A galvo steering mirror together with a 4F system was used for scanning. Collected PL light from the defect emitter passed through a bandpass filter and a confocal spatial filter and then entered the entrance slit of the monochromator. The flip mirror inside the monochromator was used to direct PL light either to a CCD camera for PL spectrum measurement or to the exit slit of the monochromator where an HBT interferometer that contains two single photon detectors (PMA hybrid 40 from Picoquant) and a correlator (Multiharp 150 from Picoquant) was used for the photon autocorrelation measurement. By twisting the exit slit width and adjusting the angle of the grating of the monochromator, different desired spectral windows can be selected to perform photon autocorrelation measurements.

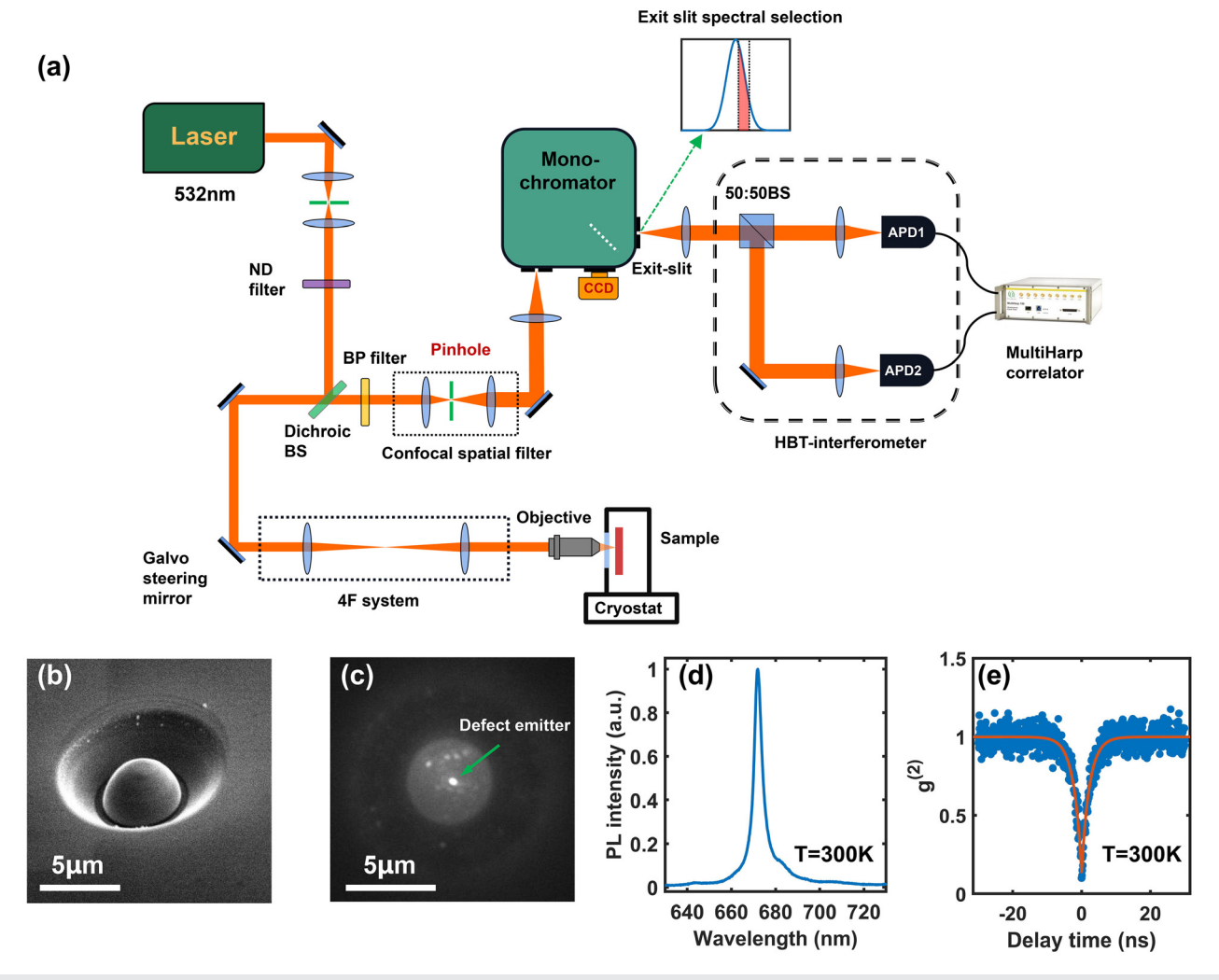


FIG. 1. (a) The layout of the custom-built confocal scanning microscope with a monochromator and a Hanbury Brown and Twiss interferometer is shown. By adjusting the exit slit width and the angle of the grating in the monochromator, different desired spectral windows of the PL spectrum of the defect emitter can be selected. (b) The SEM image of the solid immersion lens (hemisphere of diameter 5 μ m) is shown. (c) The spatial PL map of the defect emitter integrated inside the solid immersion lens is shown. (d) The PL spectrum of the defect emitter at room temperature is shown. The center wavelength is 672 nm. (e) The measured second-order correlation function [$g^{(2)}(\tau=0)=0.14$] of the defect emitter at room temperature is shown.

The defect emitters under investigation were hosted in a $4 \mu m$ thick semi-insulating GaN epitaxial layer grown using HVPE on a sapphire substrate. GaN is a high refractive index material (n \sim 2.4) in the visible wavelength range. As a result, most PL light from the defect emitter is trapped inside the substrate due to total internal reflection. To overcome total internal reflection and enhance the collection efficiency, a solid immersion lens (SIL) was fabricated on top of the defect emitter by focused ion beam (FIB) milling. ¹² The SIL is a hemisphere with a diameter of 5 μ m, as shown in Fig. 1(b) in the SEM image. To avoid ion beam deflection caused by surface charge accumulation during FIB milling, a 30 nm aluminum was sputtered on the GaN surface, and the residual aluminum after FIB milling was removed by a wet etch. The PL collection efficiency can be enhanced by a factor 4-5, and the saturation photon count rate can reach 500-800 kcps. 12 However, to ensure long-term photostability, the emitter was excited with low laser power, typically resulting in a count rate of less than 100 kcps. Figure 1(c) displays the spatial PL map of the defect emitter integrated in the center of the SIL at room temperature. Figure 1(d) shows the PL spectrum of the defect emitter at room temperature, with a center wavelength of \sim 672 nm (1845.3 meV). The measured second-order correlation function $[g^{(2)}]$ using time tagged time resolved (TTTR) mode of the Multiharp 150 instrument at room temperature is shown in Fig. 1(e), where $g^{(2)}(\tau = 0) = 0.14$ (below 0.5) confirms the SPE identity of the defect emitter.

We start our investigation by measuring the time-dependent PL spectrum of the defect emitter under an excitation laser power of 150 μ W. Figure 2(a) displays the emission spectrum over a 5-min period, with each measurement frame having an exposure time of 2 s. The averaged PL spectrum over 5 min is shown in Fig. 2(b), where the measured data can be fitted by a Gaussian curve with a center energy

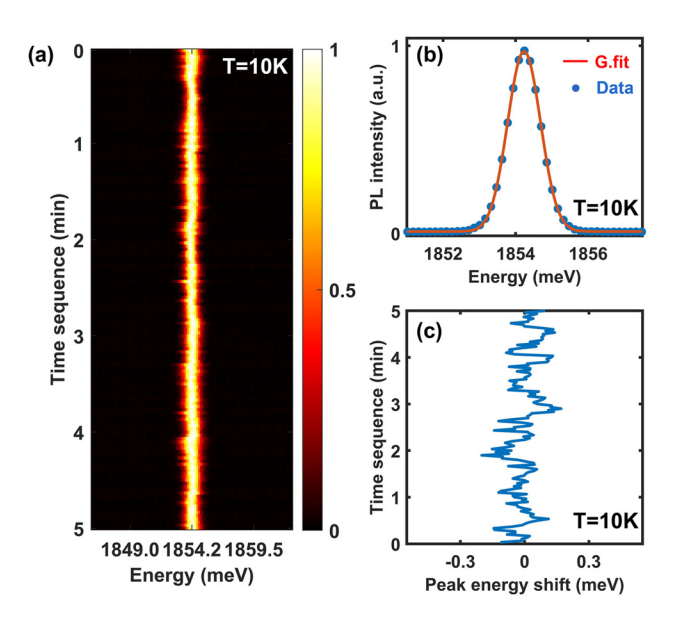


FIG. 2. (a) The time dependent PL spectrum of the defect emitter at 10 K in 5 min is shown. Each measurement frame had an exposure time of 2 s. The color bar indicates the normalized PL intensity. (b) The measured PL spectrum data averaged in 5 min at 10 K and a Gaussian fit are shown. The center energy is 1854.2 meV, and the Gaussian linewidth (FWHM) is $1.07 \, \text{meV}$. (c) The fluctuation of the fitted Gaussian center energy of each measurement frame is shown in the 5 min period.

of 1854.2 meV and a linewidth (FWHM) of 1.07 meV. A blue shift of the emission energy at low temperature is observed as reported previously, and detailed analyses of the temperature dependent linewidth and line shape can be found in earlier work. 12 Spectral diffusion caused inhomogeneous line shape at low temperature when phonon-induced linewidth broadening is negligible is known to be Gaussian, which has been observed in many other material platforms. Figure 2(c) displays the fluctuation of the fitted Gaussian center energy of each measurement frame over 5 min, and the peak energy randomly jumps within the range from -0.1 to $0.1 \,\mathrm{meV}$, with a standard deviation of 0.069 meV. This random fluctuation satisfies a Gaussian distribution, which is a typical feature of spectral diffusion. The defect emitter does not exhibit substantial spectral diffusion over a timescale of seconds, suggesting that the linewidth broadening is most likely attributed to ultrafast spectral diffusion. However, the time resolution of the spectrometer, which corresponds to the readout time of the CCD detector, limits the capture of fast dynamics below the second scale, which is more important for the characterization of ultrafast spectral diffusion. To study the ultrafast dynamics of spectral diffusion, we make use of the sub-nanosecond time resolution of the HBT interferometer and apply the photon autocorrelation measurement to the defect emitter. The angle of the grating and the exit slit width of the monochromator are carefully adjusted to select a precise spectral window of the defect emitter PL to carry out photon autocorrelation measurement.

Figure 3(a) shows that when the exit slit (indicated by the black dashed lines) is fully open to direct all the PL light of the defect emitter (pink shaded area) into the HBT interferometer, the regular antibunching effect attributed to the single photon emission nature can be

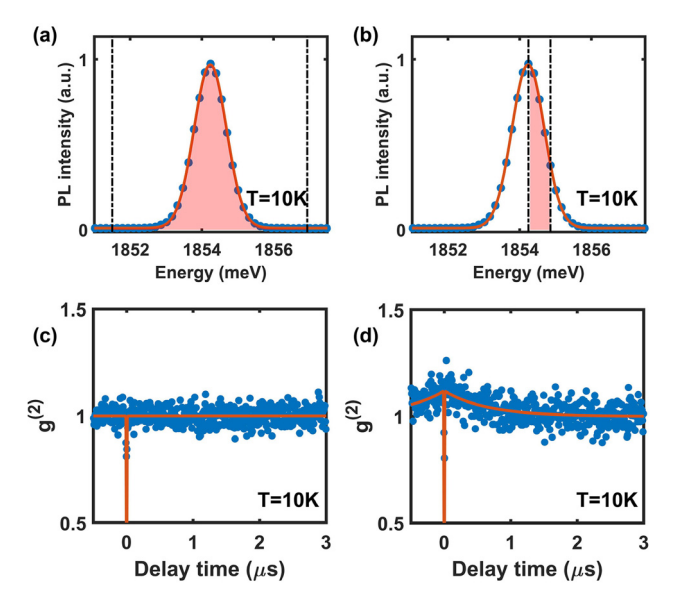


FIG. 3. (a) The spectral window selected by the exit slit of the monochromator (indicated by the black dashed lines) covers all the PL spectrum (indicated by the shaded pink area). (b) The spectral window selected by the exit slit of the monochromator (indicated by the black dashed lines) covers about one quarter of the PL spectrum (indicated by the shaded pink area). (c) The measured second-order correlation function $[g^{(2)}]$ in the case described in (a) with a laser power 150 μ W. (d) The measured second-order correlation function $[g^{(2)}]$ in the case described in (b) with a laser power 150 μ W.

observed in the measured second-order correlation function $(g^{(2)})$, as presented in Fig. 3(c). However, when the exit slit width is carefully adjusted to select a spectral window, approximately one quarter of the total PL spectrum, and direct partial PL light into the HBT interferometer as depicted in Fig. 3(b), the second-order correlation function exhibits not only the antibunching effect at zero time delay but also a bunching effect attributed to spectral diffusion. The bunching effect arises because if the time delay between two photons is large enough such that the local electric field fluctuation shifts the energy of the second photon outside the selected spectral window, a smaller $g^{(2)}$ value would be expected. Therefore, the characteristic time of the bunching effect shown in the $g^{(2)}$ function is a measure of the timescale of spectral diffusion. Since the physical property of interest here is the bunching effect (spectral diffusion), which occurs at $\sim \mu$ s, the time resolution used in the measurement is set to be 7.04 ns so that the antibunching effect is essentially averaged out as shown in Figs. 3(c) and 3(d). It is important to note that this bunching arises solely from the spectral diffusion effect, rather than the metastable state of the defect emitter, as the excitation laser power is carefully controlled (150 μ W, far below the saturation power), resulting in the absence of noticeable bunching from the metastable state, as shown in Fig. 3(c).

The measured $g^{(2)}$ data can be fitted using the function ^{19,21}

$$g^{(2)}(\tau) = \left[1 - \alpha \exp\left(-\frac{|\tau|}{\tau_e}\right)\right] \left[1 + \beta \exp\left(-\frac{|\tau|}{\tau_{SD}}\right)\right]. \tag{1}$$

Here, τ_e represents the characteristic time for the antibunching effect, while τ_{SD} represents the characteristic time for spectral diffusion. Previous works have demonstrated that the width of the selected spectral window does not affect the characteristic time of the bunching effect, but rather only its height. Figure 3(d) illustrates the characteristic time of the spectral diffusion to be $\tau_{SD}=0.64\pm0.11~\mu s$. Considering that the lifetime of the SPE estimated in Fig. 1(e) is 2.3 ns, the spectral diffusion characteristic time is two orders of magnitude longer than the emitter's lifetime. Consequently, this defect emitter can emit a few hundred indistinguishable photon wave packets before the local electric field fluctuation shifts the emission energy to other distinguishable values.

In the following discussion, we examine the dependency of the spectral diffusion rate and PL spectrum Gaussian linewidth on the excitation laser power. To ensure long-term photostability and prevent metastable state transitions from contributing to the bunching effect, the laser power is limited to a maximum of 150 μ W. Spectral diffusion is attributed to the Stark shift of the PL spectrum induced by the local electric environment fluctuation; hence, it is anticipated to be influenced by the number of excited charges in the environment, which is assumed to be proportional to the laser power.²⁹ While keeping the photon autocorrelation measurement condition described in Fig. 3(b) unchanged, the excitation laser power is varied in the range from 61 to 150 μ W. As a result, the characteristic time of the bunching effect in the $g^{(2)}$ function decreases with increasing power, as shown in Fig. 4(a). By fitting the measured data with Eq. (1), we find that the spectral diffusion rate, expressed in units of μs^{-1} (which is $1/\tau_{SD}$), exhibits a linear dependence on the excitation laser power, as shown in Fig. 4(c). This linear dependence has also been observed in other SPE platforms, such as NV centers in diamond,²⁴ quantum dots,^{20,21,23,30} and defect emitters in 2D materials like hBN. 28 This observation is consistent with the assumption that spectral diffusion is governed by

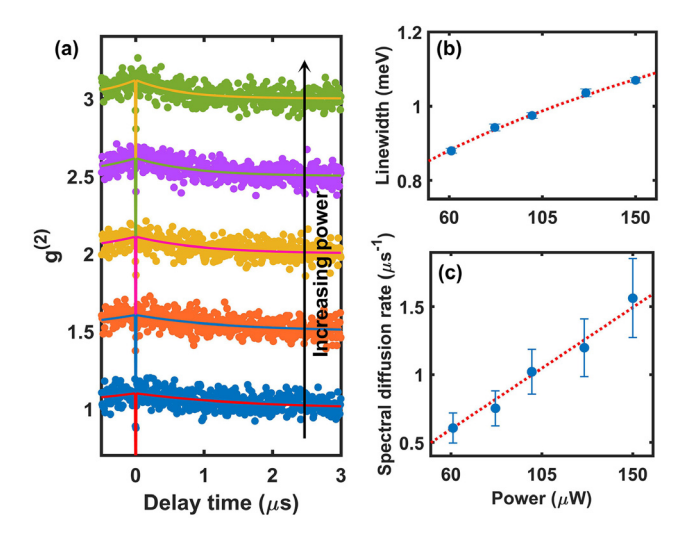


FIG. 4. (a) The excitation laser power dependent photon autocorrelation results at 10 K in the case described in Fig. 3(b) are shown. (b) The excitation laser power dependent PL spectrum Gaussian linewidth of the defect emitter is shown. (c) The excitation laser power dependent spectral diffusion rate obtained by fittings in (a) is shown.

single carrier processes rather than multiple carrier processes like Auger-assisted carrier escape from traps or two-photon processes like photoinduced charge conversion. 20,21,24 In the limit of zero laser power, the spectral diffusion rate also approaches zero, confirming the excitation laser as the primary cause of spectral diffusion. Additionally, Fig. 4(b) illustrates the relationship between the PL spectrum linewidth of the defect emitter and the laser power. As the power increases from 61 to 150 $\mu\rm W$, the linewidth only increases by about 20%, from 0.88 to 1.07 meV, and the measured linewidth data exhibit a nearly square root dependence on the laser power, which has also been reported previously in the GaN quantum dot system. 29

Spectral diffusion in SPEs limits quantum applications that demand indistinguishable photon emission. At cryogenic temperatures, the reported Gaussian linewidth of SPEs in various platforms is typically of the order ~ meV, but the measured spectral diffusion characteristic timescale for different systems varies over a relatively wide range. The characteristic time (τ_{SD}) of regular quantum dot systems is reported to be on the order of a few nanoseconds to a few hundred nanoseconds. 19-22 Nonpolar InGaN quantum dots are reported to have a maximum characteristic time of 1170 ns.²³ NV centers in diamond are reported to have a spectral diffusion characteristic time of 4.6 μs.²⁴ Defects in hBN have been reported to exhibit characteristic times of 23 μ s²⁶ and also in a range of 0.32–3.9 μ s.²⁸ In contrast, τ _{SD} in GaN defect-based SPE systems is on the order of $\sim 1 \mu s$, placing it in an intermediate region between quantum dot systems and defects in 2D materials or color centers in diamond. The bare defect SPEs in GaN can only emit a few hundred indistinguishable photon wave packets each time. Clearly, to enable more applications, integrating GaN defect SPEs into photonic cavities to harness the full potential of the Purcell effect is an important approach to overcome the limitations faced by bare SPEs.³

In conclusion, we investigated the spectral diffusion effect in both the spectral domain and the time domain of the GaN defect SPE integrated with a solid immersion lens at cryogenic temperature. Our experimental results show that the GaN defect emitter exhibits a Gaussian line shape with a linewidth of \sim 1 meV, and the spectral diffusion characteristic time falls within the range of a few hundred nanoseconds to a few microseconds. The power-dependent measurements demonstrate that the spectral diffusion rate linearly depends on the excitation laser power, while the PL spectrum Gaussian linewidth follows a nearly square root dependence on the laser power. Our work provides insight into the ultrafast spectral diffusion in GaN defect-based SPE systems.

The authors thank Professor Farhan Rana for helpful discussions. This work was supported by the Cornell Center for Materials Research with funding from the NSF MRSEC program (No. DMR-1719875) and also by the NSF-RAISE:TAQS (No. ECCS-1839196).

AUTHOR DECLARATIONS

Conflict of Interest

The authors have no conflicts to disclose.

Author Contributions

Yifei Geng: Conceptualization (lead); Investigation (lead); Writing – original draft (lead); Writing – review & editing (lead). Kazuki Nomoto: Investigation (supporting); Writing – review & editing (supporting).

DATA AVAILABILITY

The data that support the findings of this study are available from the corresponding author upon reasonable request.

REFERENCES

- ¹I. Aharonovich, D. Englund, and M. Toth, "Solid-state single-photon emitters," Nat. Photonics 10, 631–641 (2016).
- ²A. M. Berhane, K.-Y. Jeong, Z. Bodrog, S. Fiedler, T. Schröder, N. V. Triviño, T. Palacios, A. Gali, M. Toth, D. Englund *et al.*, "Bright room-temperature single-photon emission from defects in gallium nitride," Adv. Mater. 29, 1605092 (2017).
- ³A. M. Berhane, K.-Y. Jeong, C. Bradac, M. Walsh, D. Englund, M. Toth, and I. Aharonovich, "Photophysics of GaN single-photon emitters in the visible spectral range," Phys. Rev. B **97**, 165202 (2018).
- ⁴M. Nguyen, T. Zhu, M. Kianinia, F. Massabuau, I. Aharonovich, M. Toth, R. Oliver, and C. Bradac, "Effects of microstructure and growth conditions on quantum emitters in gallium nitride," APL Mater. 7, 081106 (2019).
- 5H. S. Wasisto, J. D. Prades, J. Gülink, and A. Waag, "Beyond solid-state lighting: Miniaturization, hybrid integration, and applications of GaN nano-and micro-LEDs," Appl. Phys. Rev. 6, 041315 (2019).
- ⁶S. Zhu, X. Shan, R. Lin, P. Qiu, Z. Wang, X. Lu, L. Yan, X. Cui, G. Zhang, and P. Tian, "Characteristics of GaN-on-Si green micro-LED for wide color gamut display and high-speed visible light communication," ACS Photonics 10, 92–100 (2023).
- ⁷S. P. Najda, P. Perlin, T. Suski, L. Marona, M. Leszczyński, P. Wisniewski, S. Stanczyk, D. Schiavon, T. Slight, M. A. Watson *et al.*, "GaN laser diode technology for visible-light communications," *Electronics* 11, 1430 (2022).
- ⁸C.-T. Ma and Z.-H. Gu, "Review of GaN HEMT applications in power converters over 500 W," Electronics **8**, 1401 (2019).
- ⁹E. A. Jones, F. F. Wang, and D. Costinett, "Review of commercial GaN power devices and GaN-based converter design challenges," IEEE J. Emerging Sel. Top. Power Electron. 4, 707–719 (2016).

- ¹⁰K. J. Chen, O. Häberlen, A. Lidow, C. lin Tsai, T. Ueda, Y. Uemoto, and Y. Wu, "Gan-on-Si power technology: Devices and applications," IEEE Trans. Electron Devices 64, 779–795 (2017).
- ¹¹V. Talesara, Y. Zhang, V. G. T. Vangipuram, H. Zhao, and W. Lu, "Vertical GaN-on-GaN pn power diodes with Baliga figure of merit of 27 GW/cm²," Appl. Phys. Lett. 122, 123501 (2023).
- ¹²Y. Geng, J. Luo, L. van Deurzen, H. Xing, D. Jena, G. D. Fuchs, and F. Rana, "Dephasing by optical phonons in GaN defect single-photon emitters," Sci. Rep. 13, 8678 (2023)
- ¹³Y. Geng, D. Jena, G. D. Fuchs, W. R. Zipfel, and F. Rana, "Optical dipole structure and orientation of GaN defect single-photon emitters," ACS Photonics 10(10), 3723–3729 (2023).
- 14J. Luo, Y. Geng, F. Rana, and G. D. Fuchs, "Room temperature optically detected magnetic resonance of single spins in GaN," arXiv:2306.12337 (2023).
- 15 J. Yuan, Y. Hou, Z. Yang, F. Chen, and Q. Li, "Gan as a material platform for single-photon emitters: Insights from ab initio study," Adv. Opt. Mater. 11, 2202158 (2023).
- ¹⁶C. Santori, D. Fattal, J. Vučković, G. S. Solomon, and Y. Yamamoto, "Indistinguishable photons from a single-photon device," Nature 419, 594–597 (2002).
 ¹⁷S. A. Empedocles and M. G. Bawendi, "Quantum-confined Stark effect in single
- 'S. A. Empedocles and M. G. Bawendi, "Quantum-confined Stark effect in single CdSe nanocrystallite quantum dots," Science 278, 2114–2117 (1997).
- ¹⁸H. Akbari, W.-H. Lin, B. Vest, P. K. Jha, and H. A. Atwater, "Temperature-dependent spectral emission of hexagonal boron nitride quantum emitters on conductive and dielectric substrates," Phys. Rev. Appl. 15, 014036 (2021).
- ¹⁹G. Sallen, A. Tribu, T. Aichele, R. André, L. Besombes, C. Bougerol, M. Richard, S. Tatarenko, K. Kheng, and J.-P. Poizat, "Subnanosecond spectral diffusion measurement using photon correlation," Nat. Photonics 4, 696–699 (2010).
- ²⁰K. Gao, H. Springbett, T. Zhu, R. A. Oliver, Y. Arakawa, and M. J. Holmes, "Spectral diffusion time scales in InGaN/GaN quantum dots," Appl. Phys. Lett. 114, 112109 (2019).
- ²¹K. Gao, I. Solovev, M. Holmes, M. Arita, and Y. Arakawa, "Nanosecond-scale spectral diffusion in the single photon emission of a GaN quantum dot," AIP Adv. 7, 125216 (2017).
- ²²M. Abbarchi, T. Kuroda, T. Mano, M. Gurioli, and K. Sakoda, "Bunched photon statistics of the spectrally diffusive photoluminescence of single self-assembled GaAs quantum dots," Phys. Rev. B 86, 115330 (2012).
- ²³C. Kocher, J. C. Jarman, T. Zhu, G. Kusch, R. A. Oliver, and R. A. Taylor, "Decreased fast time scale spectral diffusion of a nonpolar InGaN quantum dot," ACS Photonics 9, 275–281 (2022).
- ²⁴J. Wolters, N. Sadzak, A. W. Schell, T. Schröder, and O. Benson, "Measurement of the ultrafast spectral diffusion of the optical transition of nitrogen vacancy centers in nano-size diamond using correlation interferometry," Phys. Rev. Lett. 110, 027401 (2013).
- ²⁵L. Orphal-Kobin, K. Unterguggenberger, T. Pregnolato, N. Kemf, M. Matalla, R.-S. Unger, I. Ostermay, G. Pieplow, and T. Schröder, "Optically coherent nitrogen-vacancy defect centers in diamond nanostructures," Phys. Rev. X 13, 011042 (2023).
- ²⁶B. Spokoyny, H. Utzat, H. Moon, G. Grosso, D. Englund, and M. G. Bawendi, "Effect of spectral diffusion on the coherence properties of a single quantum emitter in hexagonal boron nitride," J. Phys. Chem. Lett. 11, 1330–1335 (2020).
- ²⁷C. Fournier, K. Watanabe, T. Taniguchi, J. Barjon, S. Buil, J.-P. Hermier, and A. Delteil, "Investigating the fast spectral diffusion of a quantum emitter in hBN using resonant excitation and photon correlations," Phys. Rev. B 107, 195304 (2023).
- ²⁸B. Sontheimer, M. Braun, N. Nikolay, N. Sadzak, I. Aharonovich, and O. Benson, "Photodynamics of quantum emitters in hexagonal boron nitride revealed by low-temperature spectroscopy," Phys. Rev. B 96, 121202 (2017).
- ²⁹M. Holmes, S. Kako, K. Choi, M. Arita, and Y. Arakawa, "Spectral diffusion and its influence on the emission linewidths of site-controlled GaN nanowire quantum dots," Phys. Rev. B 92, 115447 (2015).
- 30G. Sallen, A. Tribu, T. Aichele, R. André, L. Besombes, C. Bougerol, M. Richard, S. Tatarenko, K. Kheng, and J.-P. Poizat, "Subnanosecond spectral diffusion of a single quantum dot in a nanowire," Phys. Rev. B 84, 041405 (2011).
- 31A. Lyasota, C. Jarlov, A. Rudra, B. Dwir, and E. Kapon, "Limiting the spectral diffusion of nano-scale light emitters using the purcell effect in a photonicconfined environment," Sci. Rep. 9, 1195 (2019).
- ³²Y. Huang, R. Su, Y. Wang, C. Zhu, J. Feng, J. Zhao, Z. Liu, and Q. Xiong, "A fano cavity-photon interface for directional suppression of spectral diffusion of a single perovskite nanoplatelet," Nano Lett. 22, 8274–8280 (2022).